CSCE Annual Conference

Growing with youth – Croître avec les jeunes

Laval (Greater Montreal)

June 12 - 15, 2019

CAN A VORTEX IMPROVE FLOW CONDITIONS IN A STORMWATER RETENTION POND OR A CLEARWELL?

Chowdhury, R.[1], Mazurek, K.A.[2,4], Putz, G.[2], Albers, C.[3]
[1]City of Meadow Lake, Meadow Lake, Saskatchewan, Canada
[2]Dept. of Civil, Geological, and Environmental Engineering, University of Saskatchewan, Saskatoon, Saskatchewan, Canada
[3]Source2Source Inc., Calgary, Alberta, Canada
[4]Kerry.Mazurek@usask.ca

Abstract: Stormwater retention ponds and water treatment plant clearwells are large, open storage reservoirs a few meters in depth for which the residence time of the flow is important. For retention ponds, longer residence times provide time in the pond for settling of solids and treatment of pollutants before the stormwater is discharged into receiving waters. Clearwells need a long contact time for the disinfectant that is injected into the water flow to react before the water enters the distribution system. Both often suffer from poor flow dynamics with short-circuiting and dead space, which reduce treatment times. To improve performance, it is sometimes necessary to modify the flow behaviour, and this is often done using baffles. This paper investigates whether modifying the typical flow path in a retention pond or clearwell to a vortex can improve performance. Tests were carried out in scale models of 50 and 100 m diameter circular cells each of 2 m depth, where there was a radial inflow and a central outlet. The residence time distribution was evaluated using tracer studies for different flow rates. Observations showed that dead space was relatively small (4 and 8 % for the 50 and 100 m cells respectively), but the time of first observation of dye occurred quickly because of a secondary flow (a radial inflow near the bed towards the outlet). It appears that the secondary flow needs to be prevented for the vortex to provide a viable option for improving residence times in these types of reservoirs.

1 INTRODUCTION

Stormwater retention ponds or “wet ponds” are large, open storage reservoirs that were initially designed for flood control (Marsalek 1997). They are typically only a couple of meters in depth. These are the lakes that are aesthetic features in many Canadian neighbourhoods. However, it is known that wet ponds can also be used to help improve the quality of urban stormwater before it reaches freshwater streams (Wu et al. 1996, Marsalek and Shreier 2010). Longer residence times in these ponds improves solids retention and treatment of pollutants (Birch et al. 2006, Khan et al. 2009). Similarly, clearwells are large reservoirs, also with a flow a few metres in depth, which are used in water treatment plants as one of the last steps in the water treatment process. Disinfectant is injected into the flow near the inlet of the clearwell and a minimum contact tims is required for the disinfectant with the water before the water reaches the clearwell outlet (USEPA 1989, Crittenden et al. 2005). As such, residence time is an important concept for both stormwater retention ponds and clearwells.

Poor operational performance of wet ponds and clearwells is often due to short-circuiting and dead space in the flow (e.g., for stormwater retention ponds, see Shaw et al. 1997, Pettersson et al. 1998, and

Pettersson 1999; for clearwells, see Crozes et al. 1999). As result, baffles are often used to try and remedy poor flow conditions (for stormwater retention ponds, see Van Buren 1994; for clearwells, see Bishop et al. 1993 or Crozes et al. 1999). A potential, inexpensive alternative to using baffles is to create a large vortex in the flow by modifying the inlet and outlet piping. The long, spiral flow path of the vortex is thought to have the potential to create a long residence time for the flow in the pond. This form of flow is being used in new vortex-type stormwater pond design (Albers and Amell 2010). Instead of a "lake," the pond is a circular cell, with a radial inlet and central outlet. The pond normally has a central, circular berm to help form the vortex flow in the pond.

Herein, a simplified version of this vortex-type pond is examined through flow visualization and tracer testing in a physical scale model where the berm is not present. There are only a radial inflow and central outlet to form the vortex flow. The pond has a flat bed. Results for the flow pattern and residence time distribution for typically-sized vortex pond cells (50 m and 100 m diameter, each with a 2 m depth) are reported herein. The results should be applicable beyond the stormwater pond case to clearwells.

2 EXPERIMENTAL SETUP AND EXPERIMENTS

2.1 Experimental Setup

The experiments were conducted in a physical scale model that was operated to simulate the flow in full-scale circular cells of 50 m and 100 m diameter (at the water surface), each with depth at full-scale of 2 m. The same physical model can be used to test cells of different diameter (except for changes to the inlet and outlet piping), as the depth only needed to be varied to change the diameter to depth ratio of the pond. The outer edge of the pond had a slope of 3H:1V (i.e., the side slopes of the pond were 3H:1V) because the outer boundary of a stormwater retention pond is required to be sloped (e.g., City of Saskatoon 2017). It should be noted that this would not be so for clearwells. The inlet pipe makes a 30° angle with a tangent line to the pond circumference at the point of entrance. The inlet is oriented to cause anticlockwise vortex flow in the pond. The invert of the circular inlet pipe at full-scale is usually kept at 300 mm above the pond bed and projects a small distance into the pond. The inlet pipe has a diameter of 1.6 m for the 100 m diameter cell and 0.8 m for the 50 m diameter cell in the prototype. The central outlet is elevated so that it maintains a permanent pool in the pond. It is a circular pipe of 1.80 m diameter in the 100 m diameter cell and 1.20 m in diameter in the 50 m diameter cell. The outlet pipe extends vertically into the pond up to near the water surface. In the prototype, the outlet is closed at its top and is perforated between 50% and 75% of its total height around its circumference following the standard manhole design by Lafarge Canada Inc.

Scaling of the model followed Froude number similarity, with provisions for maintaining minimum Reynolds numbers at the inlet. Froude number similarity has been used for development of scale models of clearwells, for example by Falconer and Tebutt (1986) and Yu et al. (2010), with demonstrated capability of matching the residence time distribution observed from measurements in the prototype, even though the Reynolds numbers for the flow through the model were near the Reynolds number for transition to turbulence. Therefore, a minimum Reynolds number for the vortex flow, with the characteristic length in the Reynolds number taken as four times the hydraulic radius of the flow, was set at 2000. For the circular jet created at the inlet, a minimum Reynolds number of 3000 was used. This criterion was used because the circular turbulent jet growth has been shown to be independent of the Reynolds number in this range (Rajaratnam and Flint-Peterson 1989). Other considerations for selecting the scale for the model were the available pipe sizes for the model inlet and outlet pipes and a requirement for maintaining a depth larger than 30 mm to avoid surface tension effects on the flow (Kobus 1980). For the 100 m cell, a model scale of 1:30.775 was chosen whereas the scale for the 50 m cell was 1:13.289.

The scale model, shown in Figure 1, measured 4.393 m in diameter at its top and 2.859 mm in diameter at its base. It was 194 mm deep and constructed of 15.88 mm (5/8") marine plywood using 36 sloped, trapezoidal pieces around the circumference of the model. The model base was also constructed with plywood sheets and with a hole in the middle in order to install the central outlet pipe under it. To seal the model, the wood was painted with two coats of glossy, oil-based paint and then sealed using silicone. More details of the model construction and layout are given in Chowdhury (2016).

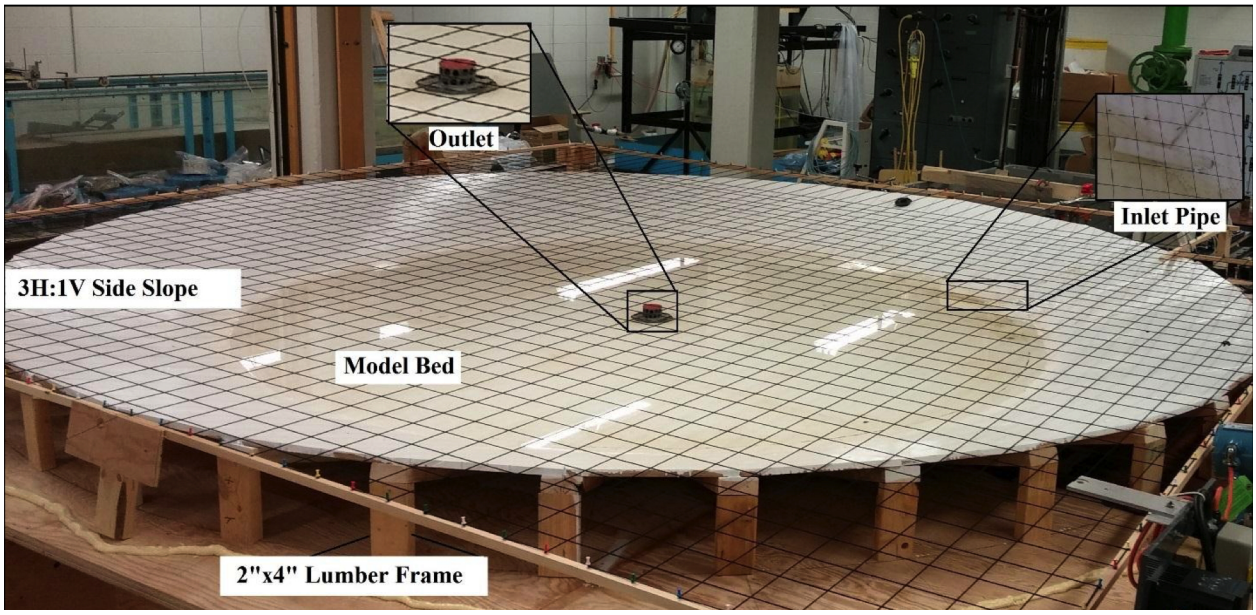

Figure 1: Physical scale model

The inside diameter of the inlet pipe was 51.5 mm for the model of the 100 m diameter cell and 61.5 mm for the model of the 50 m diameter cell. These dimensions are slightly different than the scaled diameters of the inlet pipes of 52 and 60 mm respectively due to the need to use standard PVC pipe sizes. The inlet pipe was projected about 300 mm into the model of the 100 m diameter cell and 200 mm into the model of the 50 m diameter cell. It was installed at a 30˚ angle with the tangent of the periphery at the point of entrance into the model. The inlet pipe was equipped with tracer injection and sediment injection ports, which were installed about 1.3 m upstream of the inlet to allow for complete mixing of tracer and sediments with the water before entering the model. The inlet was supplied with water by a 3 hp centrifugal pump controlled by a variable frequency drive, with a magnetic flow meter installed between the pump and inlet at the model to measure the inflow rate to the model. The water was pumped from a reservoir that with fed from a 50 mm line supplying City of Saskatoon tap water to maintain a constant head. Water was not recirculated in the model.

The outlet for the flow in the model was at the centre of the pond bed. The diameter of the outlet pipe was 58 mm and the overall outlet height was 60 mm for the model of the 100 m diameter pond. The diameter of the outlet pipe was 89 mm with an outlet height of 145 mm for the model of the 50 m diameter pond. As noted above, the outlet in a prototype pond is closed at the top and perforated between 50 and 75% of its height. This height range for perforating the outlet pipe could not be preserved for the model of the 100 m diameter cell if the desired 65 mm water level in the model was to be maintained at the design flow rate. An initial design for the perforations to pass the required outflow was constructed based on flow predictions for multiple orifice configurations available in the literature; ultimately the perforation design to maintain the desired depth was determined through trial and error. Chowdhury (2016) provides detailed sketches of the outlets used in the testing. At the flow rates other than the design flow rate, the water depth in the model could vary slightly from the equivalent depth that would occur in the prototype. The flow through the outlet moved through about a 2 m length, 38 mm diameter tube to a weir box. The weir box contained a sharp-crested V-notch weir and was equipped with a digital point gauge so that the height of water above the weir crest could be measured. The height of water above the weir was measured periodically through a test, at a distance four times the height of water above the crest of the weir, to determine the outflow rate from the model. Figure 2 shows the weir box.

The depth in the model was measured using a small diameter, 200 mm graduated tube that was installed vertically; the lower end of the tube was connected near the model bed with a small diameter pipe. The depth of the water column in the tube then indicated the flow depth in the model.

Figure 2: Weir box for the measuring the flow rate through the outlet of the model

2.2 Test Flow Conditions

For the prototype vortex-retention pond, the design flow for a 100 m cell was 4 m^3/s whereas the design flow for a 50 m cell was 1 m^3/s. These corresponded to model flows rates of 0.76 and 1.56 L/s respectively. Tests in the model 100 m cell were conducted under flow rates of 0.1, 0.4, 0.6, 0.76, and 1.0 L/s. These corresponded to 0.53, 2.10, 3.15, 4.0, and 5.25 m^3/s in the prototype. Tests in the model 50 m cell were conducted under flow rates of 0.2, 0.8, 1.2, and 1.56 L/s. These correspond to prototype values of 0.13, 0.52, and 0.77, and 1.0 m^3/s. For most flows, the inlet was fully submerged except for the 0.1 and 0.4 L/s test flow rates for the model 100 m cell and at 0.2 L/s for the model 50 m cell. The flow in the model was subcritical for all flow rates tested. Using tests with dye, it was also confirmed that the flow was turbulent in the model.

It is known from the work of Yu et al. (2010) that it can take some time for the flow to fully develop in the model before results from tracer testing are not affected by the time from initiation of flow in the model. This time is called the “flow development time”. As such, the flow development times in the model for the different flow rates tested were assessed. This was done by initiating flow in the model, waiting a particular time for the flow to develop, running a tracer test, and assessing the residence time distribution for the dye in the model. Once the residence time did not change with time of initiation of flow in the model, the flow was considered fully developed. Results from this testing is presented in Chowdhury (2016); only the results for fully developed flow are presented herein.

2.3 Tracer Testing

The residence time distribution in the flow was measured using tracer testing with slugs of Rhodamine WT dye. In a tracer test, the model was filled with water to the desired water level (the steady flow depth at the test flow rate). This was done using a hose from the City of Saskatoon tap water supply line and by closing a valve below the outlet. Next, flow through the model was initiated by setting the desired flow rate on the variable frequency drive on the pump and the valve below the outlet was opened. After the flow was allowed to develop, a slug of tracer was injected into the flow through the port in the line to the inlet using a syringe. The syringe contained 8 to 50 mL of Rhodamine WT with a concentration of 1190 or 2380 ppm. These concentrations were prepared from serial dilutions from 20% Rhodamine WT. The volume of the slug was set so that the maximum concentration reading at the outlet was not larger than 100 ppm, which was the extent of the linear range of the calibration curve of the fluorometer used for the concentration measurements.

The concentration of dye at the outlet was measured by inserting a small 4.5 mm diameter sampling tube 100 mm into the line from the outlet through the opening of this line at the upstream end of the weir box.

This sampling tube was set to sample from the centre of the cross-section of the tube from the outlet. A peristaltic pump was used to pump water from the sampling tube through a Turner Design Model 10-AU-005-CE Flow-Through Fluorometer, which was used to determine the dye concentration in the sampled flow every 2 s. The output from the fluorometer was recorded using a data acquisition system that was integrated with LabView software to record the measurements. Following the recommendation of Teefy (1996), the tracer tests were run for at least $4t_d$, where

$$[1]\ t_d = \frac{V_f}{Q}$$

where V_f is the volume of fluid in the model and Q in the flow rate through the inlet of the model. The temperature of the flow in the model was measured several times during a tracer test using a thermometer that could be read to 0.5˚C.

2.4 Flow Visualization

Flow visualization was conducted using a wireless camera suspended above the model. To aid in visualizing the flow, a 10 cm by 10 cm grid of yarn was placed above the model. The visualization used potassium permanganate or food colouring for the dye. The dye was injected into the flow using a 1 L squeeze bottle because of the large volume of dye used in the testing. Dye was injected in the inlet and pictures were taken every 2 to 3 seconds until the dye was fully distributed throughout the flow.

3 DETERMINATION OF RESIDENCE TIME PARAMETERS

The analysis of the tracer test results followed Fogler (2016), Teefy (1996), and Levenspiel (2012). In the tracer experiments, the concentration of dye, C(t), was measured at the outlet with time, t, measured from the time of appearance of the tracer in the inlet of the model. The total mass of tracer injected into the flow is M_o. The mass, ΔM_k, leaving through the outlet during time $\Delta t = t_{k+1} - t_k$ is

$$[2]\ \Delta M_k = \frac{(C_{k+1}+C_k)}{2} Q \Delta t$$

where Q is the flow rate through the system. The total mass of recovered tracer, M, is then

$$[3]\ M = \sum_{k=1}^{n-1} \Delta M_k$$

where n is the number of concentration measurements. The tracer recovery rate R can then be found:

$$[4]\ R = M/M_o$$

which is usually expressed as a percentage. For the current experiments, tracer recovery ranged from 81 to 106 %. For the residence time distribution (RTD) function, E(t), which represents the fraction of tracer mass leaving the pond with time is equal to

$$[5]\ E = \frac{C(t)}{\int_0^\infty C(t)dt} = \frac{QC(t)}{M}$$

The cumulative residence time distribution function, F(t), represents the total fraction of tracer mass that has already left the pond by a particular time t. This cumulative function F(t) is given as

$$[6]\ F(t) = \int_o^t E(t)dt$$

The residence time distribution function is not dimensionless, so instead a normalized residence time distribution function, E_θ, is used in order to compare results between tests:

$$[7]\ E_\theta = E(t)t_d$$

The normalized E_θ is plotted against the dimensionless time from the injection of the tracer at the inlet t/t_d to give the dimensionless residence time distribution curve.

From the cumulative residence time distribution curve, the percentage plug flow, mixed flow, and dead space can be calculated. These calculations were carried out following the Rebhun and Argaman (1965) model, where

$$[8]\ \ln\left(1-F\left(\frac{t}{t_d}\right)\right)=-\frac{1}{(1-P)(1-d)}\frac{t}{t_d}+\frac{P}{1-P}$$

and $F(t/t_d)$ is the cumulative residence time distribution function expressed in terms of t/t_d instead of t, P is the plug flow fraction, and d is the dead space fraction. The mixed flow fraction, m, would then be m=1-P-d. If $\ln(1-F(t/t_d)$ is calculated from the tracer test data and is plotted against t/td, it should generate a straight line. The slope of the straight line is then -1/((1-P)(1-d)) and the intercept of the vertical axis would be P/(1-P). The plug flow and dead space fractions can then be calculated from solving the equations for the slope and intercept determine from the plot.

4 RESULTS AND DISCUSSION

Figure 3 shows a comparison of the dimensionless residence time curves for the model 100 m cell at 0.76 L/s (which is equivalent to the design flow of 4 m^3/s in the prototype) and the 50 m cell at its design flow of 1.56 L/s (1 m^3/s in the prototype). It is seen that the first tracer particle arrived at the outlet more quickly for the 50 m cell than the 100 m cell. The short-circuiting index, which is the ratio of the time of first observation of the dye at the outlet, t_i, to the detention time, or t_i/t_d, was 0.04 in the 50 m cell as compared to 0.18 in the 100 m cell. The baffle factor, t_{10}/td, was also low in the 50 m cell at 0.21, while in the 100 m cell the baffle factor was 0.38. In the baffle factor, t_{10} represents the time for 10% of the mass of tracer to exit the reservoir; the baffle factor is an important parameter in the design of clearwells. The Morril dispersion index, which is the ratio of t_{90}/t_{10}, where t_{90} is the time for 90 % of the tracer mass to exit the reservoir, was 4.3 in the 100 m cell but 9.0 in the 50 m cell. A high plug flow fraction of 35 % was seen in the 100 m cell as compared to the 50 m cell at 22 %. The dead space fraction was 8 % in the 100 m cell and reduced to 4 % for the 50 m cell. The mixed flow fraction is thus 56 % in the 100 m cell and 74 % in the 50 m cell.

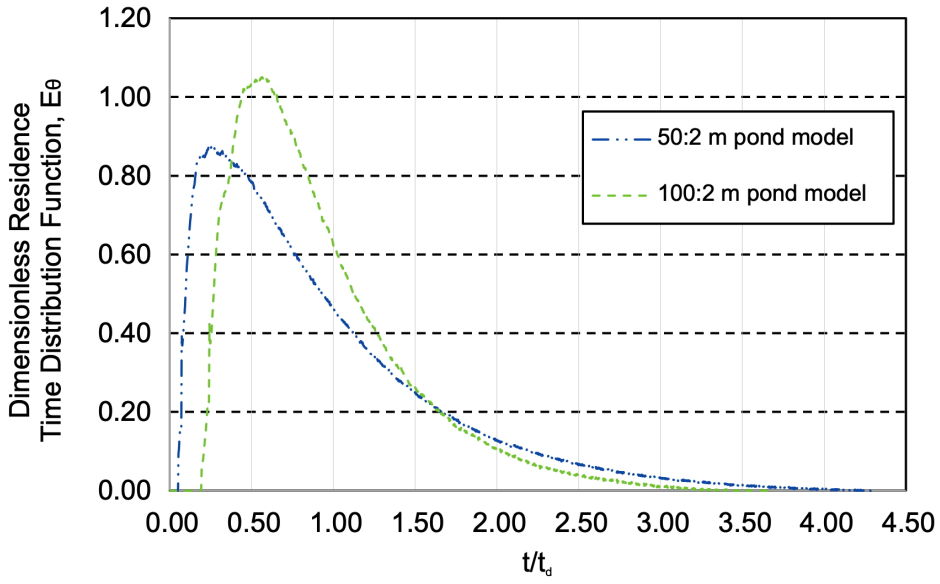

Figure 3: Comparison of the dimensionless residence time characteristics between the 100 m and 50 m cells at model flow rates of 0.76 L/s and 1.56 L/s respectively, with flow depths of 65 mm and 148 mm (both equivalent to a 2 m depth in the prototype)

Figure 4 shows the typical flow pattern in the 100 m cell, whereas Figure 5 shows the flow pattern in the 50 m cell. In both cases, the flow enters the cell and travels around the periphery of the model. It is clear that for the 100 m cell, the flow has a much longer flow path along the periphery of the cell than for the 50 m cell. The longer flow path should result in a higher fraction of plug flow; for rectangular ponds, Persson (2000) showed that the flow behaves increasingly as plug flow with increased flow path length and increasing length to width ratio of a cell. For the 50 m cell, the model showed the inflow jet filled a significant portion of the flow path, as identified through flow visualization. The width of the outer peripheral strip with the circular flow pattern was about 22 % of the radius of the cell at the flow surface for the 100 m cell, and 50 % for the 50 m cell. Hence, it can be expected that the 50 m cell has a higher mixed flow fraction than the 100 m pond.

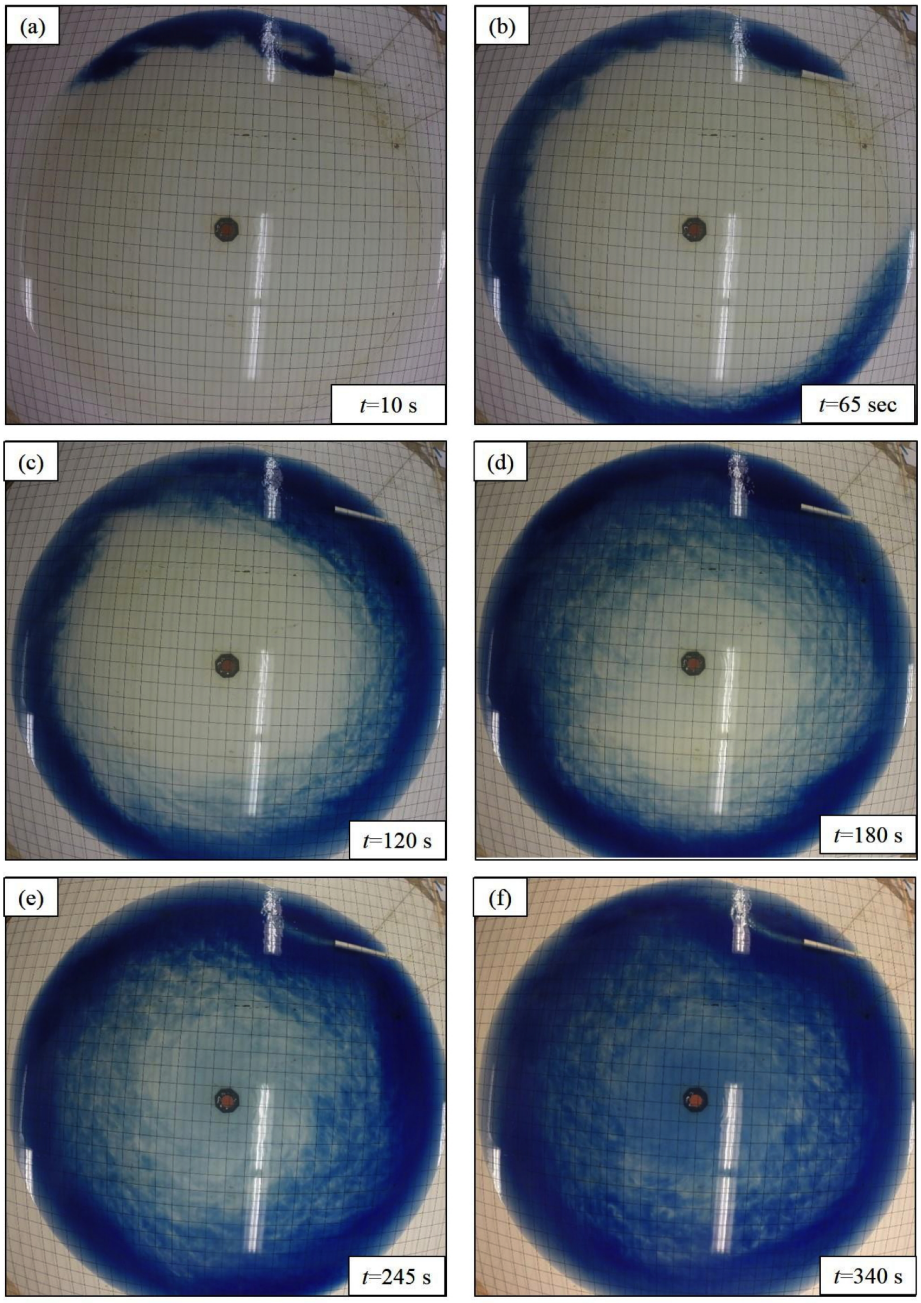

Figure 4: Flow pattern in the model of the 100 m cell at the 0.76 L/s (4 m^3/s) flow rate

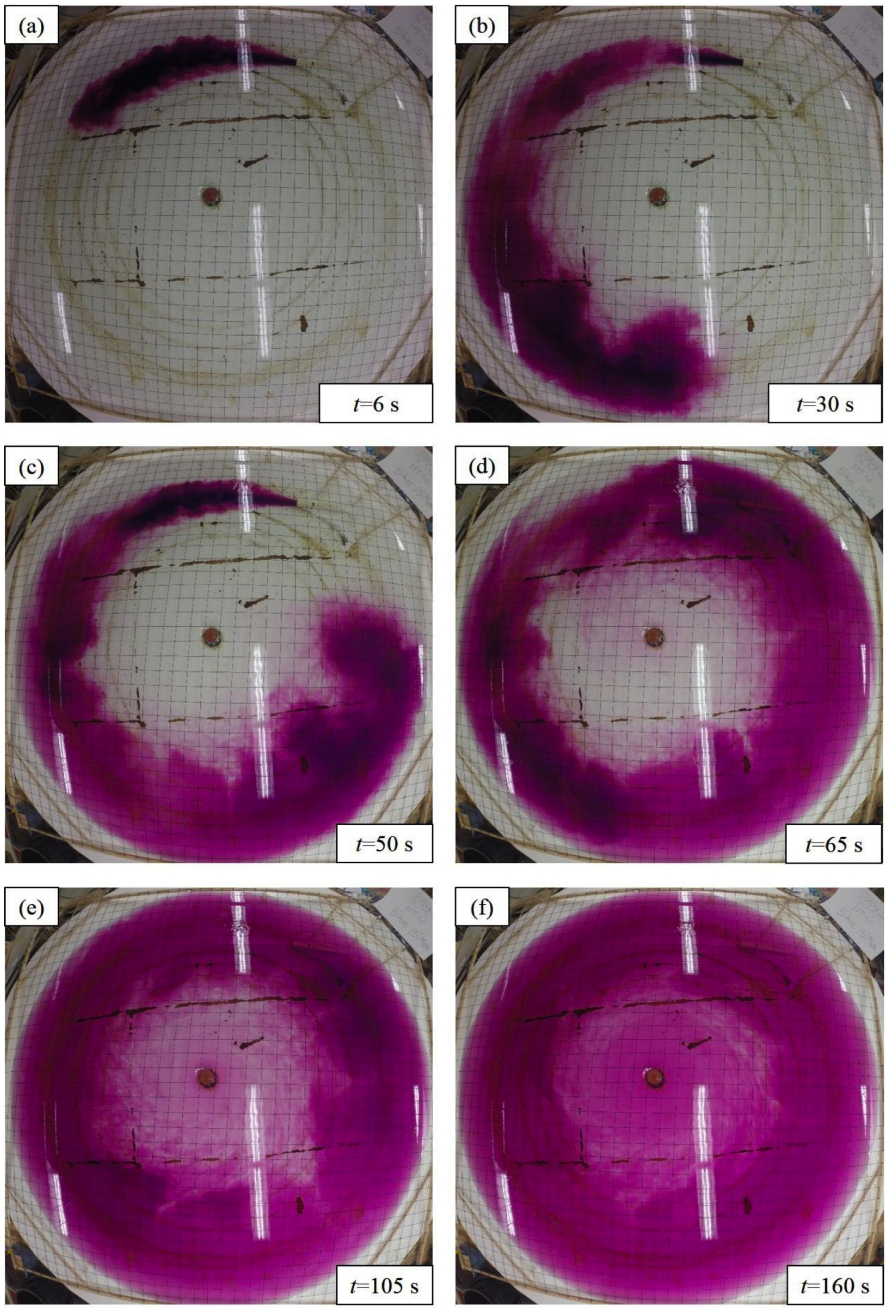

Figure 5: Flow pattern in the 50 m cell at a flow rate of 1.55 L/s (equivalent to 1 m^3/s in the prototype)

There was a radial inflow observed in both sized cells. Flow visualization showed that it was because of this secondary flow that that first observance at the outlet was much earlier than expected from a long radial flow path through the circular cell. This radial inflow moved along the bed in the lower part of the depth of flow and outwards towards the periphery in the upper part of the flow depth. The effect of this radial velocity component became more significant as the flow neared the center which created a spiral flow pattern.

The secondary radial flow may be due to a few reasons. First, the vortex at the outlet creates a depression of the water surface there. This creates a pressure gradient from the outer to inner regions of the flow. The centrifugal force due to the rotating motion of the flow also tends to create a secondary current. Finally, the inflow jet itself may drive a component of the radial inflow as the jet spreads and entrains fluid.

The influence of the flow rate on the results for the 100 m cell are shown in Table 1. In this type of configuration, the vortex pond is set to have a particular depth at the design flow and the depth of flow is lower than this design depth at lower flows and higher for higher flows. Thus, the different flow rates represent different aspect ratios (diameter to depth) for the pond. It is seen from the results that aspect ratios closer to 100:1 perform better with respect to residence time characteristics as compared to the 100:2 case. For the 100:1.1 aspect ratio there is a much longer time for first observance of the dye at the outlet and a higher baffle factor.

Table 1: Influence of flow rate on residence time distribution parameters in the 100 m cell model

Parameter	Unit	Flow Rate (L/s)				
		0.1	0.4	0.6	0.76	1.0
t_d	s	2,342	969	753	632	640
Depth of Flow	mm	34	54	52	65	84
Diameter to Depth Ratio		100:1.1	100:1.7	100:1.9	100:2	100:2.5
t_i/td		0.28	0.20	0.18	0.18	0.10
t_{10}/td		0.40	0.36	0.36	0.38	0.30
t_{10}/t_{90}		4.1	4.3	4.7	4.3	6.2

5 DISCUSSION AND CONCLUSION

For a clearwell, a superior baffle factor (t_{10}/t_d) is 0.7 while a baffle factor of 0.1 is considered “unbaffled” and 0.3 is considered poor (USEPA 1990). Therefore, the vortex cell of this configuration is performing poorly with respect to required baffle factors for clearwells. The problem appears to be the secondary flow that forms in the flow that has an inward component of velocity along the bed that quickly carries dye towards the inlet. If using a vortex in either a clearwell or as a stormwater pond is to be effective, then the inward velocity must be prevented.

ACKNOWLEDGMENTS

The authors gratefully acknowledge support for this project from the Natural Sciences and Engineering Research Council of Canada in the form of a Strategic Project Grant (STPGP428778-12) to the second and third authors. The authors also acknowledge support from department technicians Dale Pavier and Brennan Pokoyoway in constructing and ensuring the operation of the experimental setup, as well as departmental assistant Adam Hammerlindl for his input in developing the design of the setup.

REFERENCES

Albers, C. and Amell, B. 2010. Changing the stormwater pond design game. *Proc. 10th NOVATECH Conference*, GRAIE, Lyon, France.

Birch, G.F., Matthai, C., and Fazelli, M.S. 2006. Efficiency of a retention/detention basin to remove contaminants from urban stormwater. *Urban Water Journal*, **3**(2): 69-77.
Bishop, M.M., Morgan, J.M., Cornwell, B., and Jamison, D.K. 1993. Improving the disinfection detention time of a water plant clearwell. *J. AWWA, Research and Technology*, March: 69-75
Chowdhury, R. 2016. Assessment of Flow Conditions in a New Vortex-Type Stormwater Retention Pond using a Physical Model. M.Sc. Thesis, Dept. of Civil and Geological Engineering, University of Saskatchewan, Saskatoon, Saskatchewan.
City of Saskatoon 2007. *City of Saskatoon Design and Development Standards Manual: Section Six – Storm Water Drainage System*. City of Saskatoon, Saskatoon, Saskatchewan, Canada.
Crittenden, J.C., Trussell, R.R., Hand, D.W., and Tchobanoglous, G. 2005. *Water Treatment Principles and Design (2nd Edition*). John Wiley and Sons, Hoboken, New Jersey, USA.
Crozes, G.F., Hagstrom, J.P., Clark, M.M., Ducoste, J., and Burns, C. 1999. *Improving Clearwell Design for CT Compliance*. American Water Works Association Research Foundation, Denver, Colourado, USA.
Falconer, R.A., and Tebbutt, T.H.Y. 1986. A theoretical and hydraulic model study of a chlorine contact tank. *Proceedings of the Institution of Civil Engineers, Part 2*, **81**(6): 255–276.
Fogler, H.S. 2016. Residence time distributions of chemical reactors. *Elements of Chemical Reaction Engineering, 5th edition*, Pearson Education Inc., Boston, Massachusetts, USA.
Khan, S., Melville, B.W., Shamseldin, A.Y. 2009. Modeling the layouts of stormwater retention ponds using residence time. *Proc. of the 4th IASME/WSEAS Int. Conf. on Water Resources, Hydraulics and Hydrology (WHH'09),* WEAS, Cambridge, UK, 77-83.
Kobus, H. 1980. *Hydraulic Modeling*. Pitman Publishing Inc., Marshfield, Massachusetts, USA.
Levenspiel, O. 2012. *Tracer Technology: Modeling the Flow of Fluids*. Springer, New York, NY, USA.
Marsalek, J., and Schreier, H. 2010. Innovation in stormwater management in Canada: The way forward. *Water Quality Research Journal of Canada*, **44**(1): v-x.
Marsalek, P.M. 1997. *Special Characteristics of An On-Stream Stormwater Management Pond: Winter Regime and Accumulation of Sediment and Associated Contaminants*. M.Sc. Thesis, Department of Civil Engineering, Queen's University, Kingston, Ontario, Canada.
Persson, J. 2001. The hydraulic performance of ponds of various layouts. *Urban Water*, **2**(3), 243-250.
Pettersson, T.J.R. 1999. *Stormwater Ponds for Pollution Reduction*. Ph.D. Thesis, Dept. of Sanitary Engineering, Chalmers University of Technology, Göteborg, Sweden.
Pettersson, T.J.R., German, J., and Svensson, G. 1998. Modelling of flow pattern and particle removal in an open stormwater detention pond. *Proc. Hydrostorm '98*, Adelaide, Australia, 63-68.
Rajaratnam, N. and Flint-Peterson, L. 1989. Low Reynolds number circular turbulent jets. *Proceedings-Institution of Civil Engineers, Part 2: Research and Theory*, **87**: 299-305.
Rebhun, M., and Argaman, Y. 1965. Evaluation of hydraulic efficiency of sedimentation basins. *Journal of the Sanitary Engineering Division*, *Proceedings of the American Society of Civil Engineers*, **91**(SA5), 37–45.
Shaw, J.K.E., Watt, W.E., Marsalek, J., Anderson, B.C., and Crowder, A.A. 1997. Flow pattern characterization in an urban stormwater detention pond and implications for water quality. *Water Quality Research Journal of Canada*, **32**(1): 53-71.
Teefy, S. 1996. *Tracer Studies in Water Treatment Facilities: A Protocol and Case Studies*. AWWA Research Foundation, American Water Works Association, Denver, Colourado, USA.
USEPA (United States Environmental Protection Agency). 1989. *Guidance Manual for Compliance with the Filtration and Disinfection Requirements for Public Water Systems using Surface Water Sources*. USEPA, Washington, D.C., USA.
USEPA (United States Environmental Protection Agency). 1990. *Guidance Manual for Compliance with the Filtration and Disinfection Requirements for Public Water Systems using Surface Water Sources*. USEPA, Washington, D.C., USA.
Van Buren, M.A. 1994. *Constituent Mass Balance for an Urban Stormwater Detention Pond in Kingston Township*. M.Sc.Thesis, Dept. of Civil Engineering, Queen's University, Kingston, Ontario, Canada.
Wu, J.S., Holman, R.E., and Dorney, J.R. 1996. Systematic evaluation of pollutant removal by urban wet detention ponds. *J. Environmental Engineering*, 122(11): 983-988.
Yu, X., Mazurek, K.A., Putz, G., and Albers, C. 2010. Physical and computational modelling of residence and flow develop time in a large municipal disinfection clearwell. *Canadian J. Civil Engineering*, **37**: 931–940.